IV International Conference on Computational Methods for Coupled Problems in Science and Engineering
COUPLED PROBLEMS 2011
M. Papadrakakis, E. Oñate and B. Schrefler (Eds)

THE INFLUENCE OF DIFFERENT TIME INTEGRATION SCHEMES IN ALE DESCRIPTION APPLIED TO MOVING MESHES

FRANK FLITZ*†, DÖRTE C. STERNEL* AND MICHAEL SCHÄFER*

*Institute of Numerical Methods in Mechanical Engineering
Technische Universität Darmstadt
Dolivostraße 15, 64293 Darmstadt, Germany
e-mail: {flitz,sternel,schaefer}@fnb.tu-darmstadt.de, http://www.fnb.tu-darmstadt.de

†Graduate School of Computational Engineering
Technische Universität Darmstadt
Dolivostraße 15, 64293 Darmstadt, Germany
e-mail: flitz@gsc.tu-darmstadt.de, http://www.graduate-school-ce.de

Key words: Time Discretization, Arbitrary Lagrangian Eulerian, Moving Mesh

Abstract. We analyze the error introduced by the arbitrary Lagrangian Eulerian description on a deliberately moved mesh with a flow field which is steady in Eulerian description. As governing equations, the Navier-Stokes equations for incompressible flow are considered. Two different discretization concepts are investigated for two time integration schemes. It turns out that the difference between the concepts is rather small, but that the difference in the time integration schemes and the dependency of the grid CFL number is much larger.

1 INTRODUCTION

Especially in the context of transient fluid-structure interaction the computational domain of the flow changes with time. When the computational grid is adapted in each time step, it is expensive to interpolate field variables in Eulerian description from one time instance to the next. The arbitrary Lagrangian Eulerian (ALE) description is an elegant extension to the Eulerian description that eliminates the need for this interpolation.

The main question we address is: What error is introduced to a solution which is steady in Eulerian description when it is calculated unsteadily in ALE description. For uniform flow similar tests were already performed in [1] to check for the fulfillment of the space conservation law.

In section 2 we introduce the basic equations for dealing with the ALE description followed by the problem specification in section 3 and the description of the methods

employed in section 4. The test cases and the corresponding results are shown in section 5.

2 BASIC EQUATIONS

The governing equations in ALE description are obtained via minor changes to the ones in Eulerian description. These changes manifest themselves in a time derivative over a time dependent control volume (CV) and a correction to the convective velocity in terms of a grid velocity.

The substantial derivative can be denoted in the Eulerian and in the ALE description as:

$$\frac{\mathrm{d}\phi}{\mathrm{d}t} = \frac{\partial\phi}{\partial t} + \boldsymbol{u}\cdot\nabla\phi = \left.\frac{\partial\phi}{\partial t}\right|_{\mathrm{ALE}} + (\boldsymbol{u}-\boldsymbol{u}^{\mathrm{g}})\cdot\nabla\phi\,. \tag{1}$$

Here the term on the left hand side is the substantial derivative of some generic variable ϕ with respect to time t. $\frac{\partial\phi}{\partial t}$ is the Eulerian time derivative and $\boldsymbol{u}$ is the material velocity

$$\boldsymbol{u} = \frac{\mathrm{d}\boldsymbol{x}}{\mathrm{d}t} \tag{2}$$

with the spatial coordinate $\boldsymbol{x}$. The grid velocity

$$\boldsymbol{u}^{\mathrm{g}} = \left.\frac{\partial\boldsymbol{x}}{\partial t}\right|_{\mathrm{ALE}}\,. \tag{3}$$

appears on the right hand side of (1). For incompressible flow, which is assumed here, the Navier-Stokes equations with the assumption of a Newtonian fluid and no external body force in Eulerian description read as follows:

$$\nabla\cdot\boldsymbol{u} = 0\,, \tag{4}$$

$$\rho\frac{\partial\boldsymbol{u}}{\partial t} + \rho\boldsymbol{u}\cdot\nabla\boldsymbol{u} + \mu\nabla^2\boldsymbol{u} - \nabla p = 0 \tag{5}$$

with the density ρ, the dynamic viscosity μ, and the pressure p. With the change to the ALE description the momentum equation changes correspondingly to (1), while the continuity equation remains the same due to the incompressibility assumption:

$$\nabla\cdot\boldsymbol{u} = 0\,, \tag{6}$$

$$\rho\left.\frac{\partial\boldsymbol{u}}{\partial t}\right|_{\mathrm{ALE}} + \rho\,(\boldsymbol{u}-\boldsymbol{u}^{\mathrm{g}})\cdot\nabla\boldsymbol{u} + \mu\nabla^2\boldsymbol{u} - \nabla p = 0\,. \tag{7}$$

For the application of a finite-volume method the Navier-Stokes equations have to be rewritten in integral form. These change from the Eulerian description

$$\int_S \boldsymbol{u}\cdot\boldsymbol{n}\,\mathrm{d}S = 0\,, \tag{8}$$

$$\frac{\partial}{\partial t}\int_V \rho\boldsymbol{u}\,\mathrm{d}V + \int_S \rho\boldsymbol{u}\boldsymbol{u}\cdot\boldsymbol{n}\,\mathrm{d}S + \mu\int_S \nabla\boldsymbol{u}\cdot\boldsymbol{n}\,\mathrm{d}S - \int_V \nabla p\,\mathrm{d}V = \boldsymbol{0} \tag{9}$$

with $\boldsymbol{n}$ being the face normal vector, to the ALE description

$$\int_S \boldsymbol{u} \cdot \boldsymbol{n} \, \mathrm{d}S = 0 \,, \tag{10}$$

$$\left.\frac{\partial}{\partial t}\right|_{\mathrm{ALE}} \int_V \rho \boldsymbol{u} \, \mathrm{d}V + \int_S \rho \boldsymbol{u} \left(\boldsymbol{u} - \boldsymbol{u}^{\mathrm{g}}\right) \cdot \boldsymbol{n} \, \mathrm{d}S + \mu \int_S \nabla \boldsymbol{u} \cdot \boldsymbol{n} \, \mathrm{d}S - \int_V \nabla p \, \mathrm{d}V = \boldsymbol{0} \,. \tag{11}$$

For further details about the ALE description see for instance [2].

3 PROBLEM SPECIFICATION

We address the following question: What error is introduced to a solution which is steady in Eulerian description when it is calculated unsteadily in ALE description?

Similar tests were already performed for uniform flow ([1], [3]). Exactly resampling a uniform flow is a consequence of the fulfillment of the space conservation law ([1]) or geometric conservation law ([4]), as it is called moreoften. As it was shown in [3] this law is a necessary and sufficient condition for the time integration scheme in ALE description being as stable as the corresponding scheme in Eulerian description.

Since we calculate the grid velocity implicitly corresponding to the space conservation law our focus lies on the discretization of the time derivative term

$$\left.\frac{\partial}{\partial t}\right|_{\mathrm{ALE}} \int_V u \, \mathrm{d}V \,. \tag{12}$$

We examine its influence on a flow with a gradient in the direction of the grid movement, but we do not determine the accuracy of the time integration in ALE description itself, as it is done in [5].

Two concepts for dicretizing the time derivative are introduced in the next section. For the sake of simplicity only 1d and quasi-1d configurations are considered.

4 METHODS

Before discretizing (12) in time it is discretized in the ALE domain according to the midpoint rule, yielding:

$$\left.\frac{\partial}{\partial t}\right|_{\mathrm{ALE}} \int_V u \, \mathrm{d}V \approx \left.\frac{\partial}{\partial t}\right|_{\mathrm{ALE}} (u \delta V) \,. \tag{13}$$

The two obvious ways to discretize this term are: *Concept A:* treat $u\delta V$ as one term and: *Concept B:* treat u and δV as two distinct terms.

For time integration we use the implicit Euler (EI) scheme and the second order backward differencing (BDF2) scheme. Applying concept A to the EI scheme yields

$$\left.\frac{\partial}{\partial t}\right|_{\mathrm{ALE}} \int_V u \, \mathrm{d}V \approx \frac{1}{\Delta t} \left(u^{n+1} \delta V^{n+1} - u^n \delta V^n\right) \tag{14}$$

with Δt being the constant time interval, $n+1$ indicating the current time instance and n the old one. Applying concept B yields

$$\begin{aligned}\left.\frac{\partial}{\partial t}\right|_{\mathrm{ALE}} \int_V u \,\mathrm{d}V &\approx \left.\frac{\partial}{\partial t}\right|_{\mathrm{ALE}} (u)\,\delta V + u \left.\frac{\partial}{\partial t}\right|_{\mathrm{ALE}} (\delta V) \\ &\approx \frac{1}{\Delta t}\left(\left(u^{n+1}-u^n\right)\delta V^{n+1} + u^{n+1}\left(\delta V^{n+1}-\delta V^n\right)\right) \\ &= \frac{1}{\Delta t}\left(u^{n+1}\left(2\delta V^{n+1}-\delta V^n\right) - u^n \delta V^{n+1}\right)\end{aligned} \tag{15}$$

with $n-1$ the second last time instance. Applied to the BDF2 scheme concept A and concept B give

$$\left.\frac{\partial}{\partial t}\right|_{\mathrm{ALE}} \int_V u \,\mathrm{d}V \approx \frac{1}{\Delta t}\left(\frac{3}{2}u^{n+1}\delta V^{n+1} - 2u^n\delta V^n + \frac{1}{2}u^{n-1}\delta V^{n-1}\right) \tag{16}$$

and

$$\begin{aligned}\left.\frac{\partial}{\partial t}\right|_{\mathrm{ALE}} \int_V u \,\mathrm{d}V &\approx \left.\frac{\partial}{\partial t}\right|_{\mathrm{ALE}} (u)\,\delta V + u \left.\frac{\partial}{\partial t}\right|_{\mathrm{ALE}} (\delta V) \\ &\approx \frac{1}{\Delta t}\left(\left(\frac{3}{2}u^{n+1} - 2u^n + \frac{1}{2}u^{n-1}\right)\delta V^{n+1}\right. \\ &\quad \left. + u^{n+1}\left(\frac{3}{2}\delta V^{n+1} - 2\delta V^n + \frac{1}{2}\delta V^{n-1}\right)\right) \\ &= \frac{1}{\Delta t}\left(u^{n+1}\left(3\delta V^{n+1} - 2\delta V^n + \frac{1}{2}\delta V^{n-1}\right)\right. \\ &\quad \left. -2u^n\delta V^{n+1} + \frac{1}{2}u^{n-1}\delta V^{n+1}\right),\end{aligned} \tag{17}$$

respectively.

5 NUMERICAL INVESTIGATIONS

The influence of the two concepts is analyzed for three test cases. The test cases concern flows varying in the direction of the grid movement. As a first test case a manual calculation on a concrete example flow is considered. The second test case has the aim to check the implementation and the validity of the boundary conditions. Finally, the third test case examines a general nonlinear flow.

The numerical simulations are carried out with the finite-volume code FASTEST ([6]), which is based on hexahedral block structured grids and uses a pressure-correction scheme with the SIMPLE algorithm. The discrete system is solved via a geometric multigrid method incorporating the incomplete LU decomposition method by Stone as a smoother. The fluxes are discretized via central differences. For the fine grid in the channel flow configuration (see section 5.3) 6 grid levels are used. The space conservation law is fulfilled implicitly as proposed in [1].

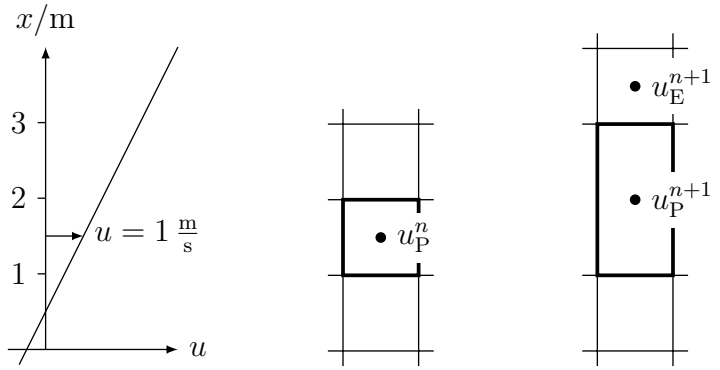

(a) velocity profile (b) undeformed (c) deformed

Figure 1: Velocity profile and configuration for the manual calculation

5.1 Manual test case

The manual calculations are conducted on a segment with three adjoining CVs immersed in a Couette flow (see Figure 1a). The extension of the CVs in the two directions orthogonal to the velocity gradient can be deliberately chosen, but is equal for all CVs and constant in time (see Figure 1b). Therefore this is a quasi 1d configuration. Constant pressure is assumed.

In order to judge whether a flow with a CV size change in ALE description will give the same result as the steady Eulerian solution, singly the time derivative and the grid velocity part of the convective term have to be considered. Therefore, the momentum equation in Eulerian description (9) in steady form is subtracted from the momentum equation in ALE description (11), yielding:

$$\left.\frac{\partial}{\partial t}\right|_{\mathrm{ALE}} \int_V \rho \boldsymbol{u}\,\mathrm{d}V - \int_S \rho \boldsymbol{u}\boldsymbol{u}^{\mathrm{g}} \cdot \boldsymbol{n}\,\mathrm{d}S = \boldsymbol{0}\,. \tag{18}$$

This equation has to be fulfilled for switching between the undeformed and the deformed configuration. We test this for the EI scheme in 1d on the configuration displayed in Figure 1. The time step size Δt is set to 1 s and the density ρ is $1\,\frac{\mathrm{kg}}{\mathrm{m}^3}$. Concept A results in

$$\begin{aligned}
&\left.\frac{\partial}{\partial t}\right|_{\mathrm{ALE}} \int_V \rho u\,\mathrm{d}V - \int_S \rho u u^{\mathrm{g}}\,\mathrm{d}S \\
&\approx \frac{\rho}{\Delta t}\left(u_{\mathrm{P}}^{n+1}\delta V^{n+1} - u_{\mathrm{P}}^{n}\delta V^{n}\right) - \frac{\rho}{\Delta t}\left(\delta V^{n+1} - \delta V^{n}\right)\left(\frac{1}{3}u_P^{n+1} + \frac{2}{3}u_{\mathrm{E}}^{n+1}\right) \\
&= -0.5\,\frac{\mathrm{kg\,m}}{\mathrm{s}^2} \neq 0
\end{aligned} \tag{19}$$

and concept B yields

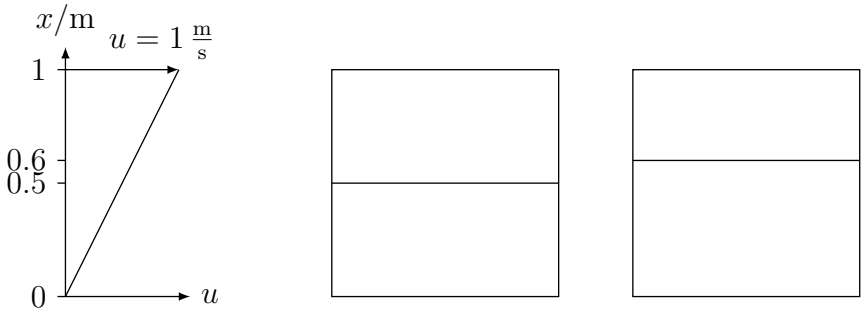

(a) velocity profile (b) undeformed (c) deformed

Figure 2: Velocity and CVs for the linear test case

$$
\begin{aligned}
&\left.\frac{\partial}{\partial t}\right|_{\mathrm{ALE}} \int_V \rho u \,\mathrm{d}V - \int_S \rho u u^{\mathrm{g}} \,\mathrm{d}S \\
&\approx \frac{\rho}{\Delta t}\left(u_{\mathrm{P}}^{n+1}\left(2\delta V^{n+1} - \delta V^n\right) - u_{\mathrm{P}}^n \delta V^{n+1}\right) \\
&\quad - \frac{\rho}{\Delta t}\left(\delta V^{n+1} - \delta V^n\right)\left(\frac{1}{3}u_P^{n+1} + \frac{2}{3}u_{\mathrm{E}}^{n+1}\right) \\
&= 0\,.
\end{aligned}
\tag{20}
$$

As we can see, concept A fails, while concept B passes this simple test.

5.2 Linear test case

In the finite-volume solver FASTEST, both concepts are tested on a Couette flow with two CVs in order to test the implementation. The two CVs span an area of $1\,\mathrm{m} \times 1\,\mathrm{m} \times 1\,\mathrm{m}$. At the beginning of the simulation both CVs have an extension of 0.5 m in the wall normal direction, which increases to 0.6 m for the lower one and decreases to 0.4 m for the upper one correspondingly (see Figures 2b and 2c).

The velocity of the lower wall is 0 and of the upper wall is $1\,\frac{\mathrm{m}}{\mathrm{s}}$. In the directions orthogonal to the wall normal direction periodic boundary conditions are applied. For the viscosity a small but finite value ($\mu = 1 \times 10^{-8}\,\frac{\mathrm{kg}}{\mathrm{s\,m}}$) is used to avoid diffusion effects weakening the errors introduced by the schemes.

We obtain results confirming the observations of section 5.1. The converged solution with concept A is erroneous, while concept B gives the exact result.

5.3 Nonlinear test case

As a nonlinear test case a flow between two flat plates is considered. The calculation domain is a cube with edge length 1 m, which is splitted in wall normal direction into 4 blocks of equal size (Figure 3b) with 32 equally spaced CVs in each direction for the fine grid, giving a total number of 131 072 CVs. The boundary conditions are given by no slip

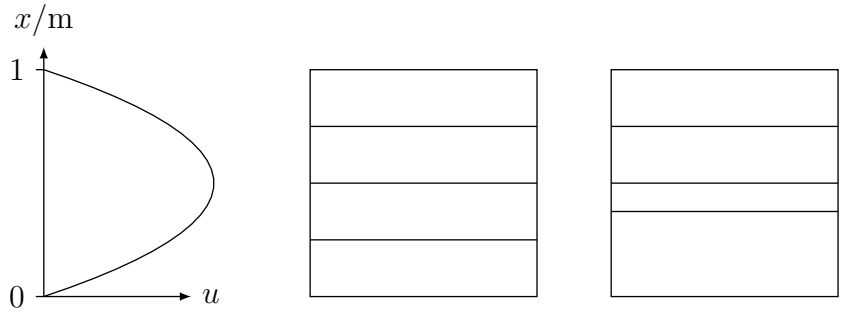

(a) velocity profile (b) undeformed (c) fully deformed

Figure 3: Velocity and blocks for nonlinear test case

walls and periodic conditions in the other two directions. The flow is driven by a pressure gradient of $1.2 \times 10^{-7} \frac{\mathrm{Pa}}{\mathrm{m}}$ applied as a body force. Together with a dynamic viscosity of $1 \times 10^{-8} \frac{\mathrm{kg}}{\mathrm{s\,m}}$ this yields a maximal velocity of $1.5 \frac{\mathrm{m}}{\mathrm{s}}$. The density is equal to $1 \frac{\mathrm{kg}}{\mathrm{m}^3}$.

During the computation the interface between the lowest block and its neighboring one is shifted by one eighth of the plate clearance towards the middle of the domain (see Figure 3c). The CVs in each of the two blocks are uniformly expanded and compressed, respectively. The other two blocks stay unmodified. As initial solution for the calculation the converged solution of the undeformed grid is used.

The following four parameters are varied:

- Time integration scheme,
- Grid resolution (see Table 1),
- Displacement velocity,
- Time step size.

Our calculations show that regarding the error a increase in the displacement velocity can be eliminated by a decrease in time step size and vice versa. Therefore these two parameters are replaced by a new one: Displacement steps. The full displacement is kept constant, as displayed in Figure 3c. Only the number of equally distributed displacement steps to achieve this full displacement is of interest.

We examine the error in the velocity component parallel to the pressure gradient after the full displacement. It is calculated as the CV size weighted L_2-norm of the difference between the solution right after the full displacement and the steady solution on the fully deformed grid. The results are shown in Figure 4. The difference between the concepts

Table 1: Grid levels for the nonlinear test case

Grid	Control volumes
fine	131 072
medium	16 384
coarse	2048

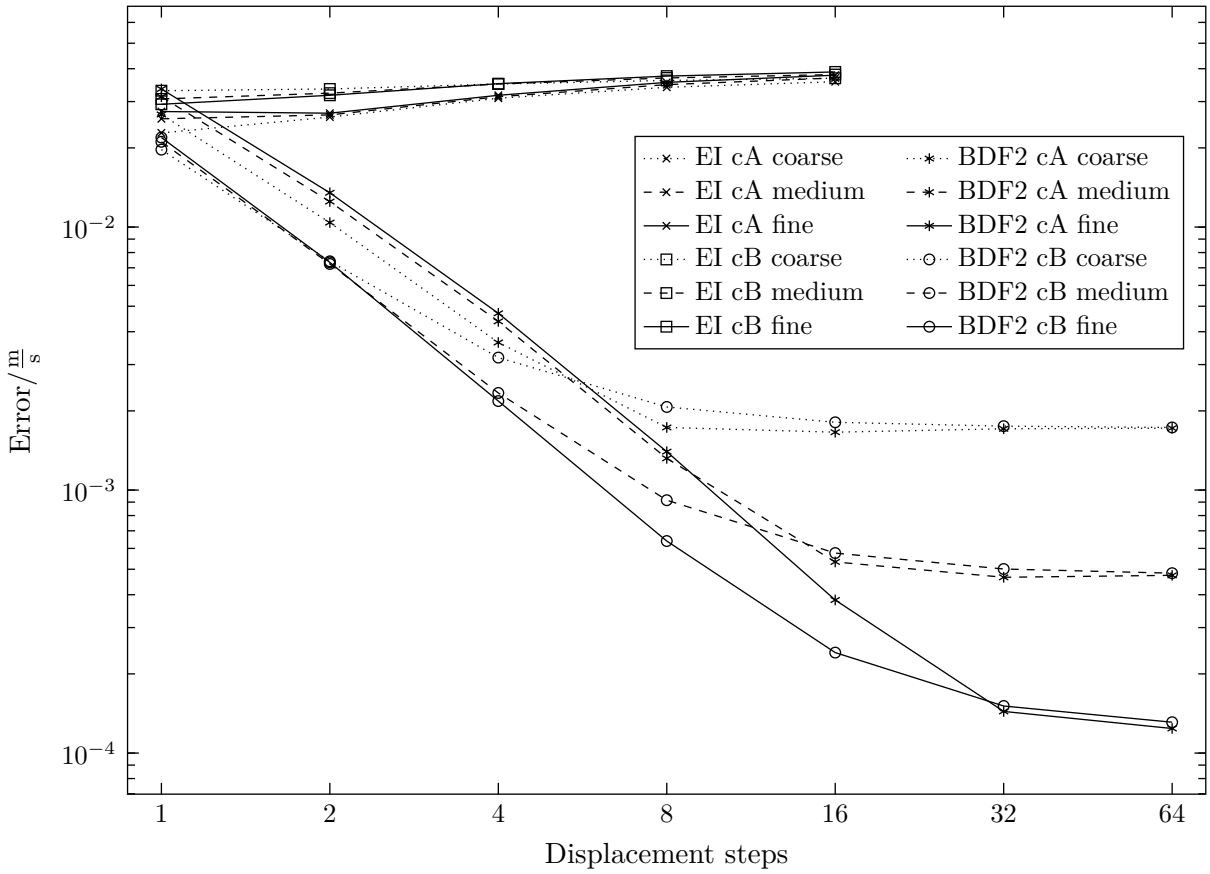

Figure 4: Errors for the nonlinear test case. cA denotes concept A and cB concept B.

is rather small in comparison to the difference between the schemes.

For the EI scheme there is no significant difference between the concepts. However, for the BDF2 scheme the error for concept A is about twice the error of concept B for a small number of displacement steps. For a large number of displacement steps there is also no significant difference.

While for the EI scheme the error is nearly independent of the number of displacement steps, the error of the BDF2 scheme shows a characteristic change between the behavior for a small and a large number of displacement steps. For the BDF2 scheme with a small number of displacement steps a decrease of the error with increasing number of displacement steps of the order of about 1.5 can be seen. For a large number of displacement steps the error stays nearly constant. The change between these two behaviors happens at a grid dependent number of displacement steps. In order to describe this behavior the grid CFL number ν^{g} is introduced:

$$\nu^{\mathrm{g}} = \frac{u^{\mathrm{g}} \Delta t}{\Delta x} \,. \tag{21}$$

For example, 16 displacement steps on the fine grid result in a grid CFL number of 1 at the beginning of the computation, while due to the decreasing CV size within the computation, the grid CFL number increases gradually to a value of 2 at the end of the computation. The intersection of the two asymptotes the error approaches for small and large numbers of displacement steps is in the vicinity of an average grid CFL number of 1. Generally, this is true for all grid levels.

6 CONCLUSIONS

Although the results from the linear test case induce the conclusion that the two considered discretization concepts have significant influence on the error, the results from the nonlinear test case show that this difference is negligible in contrast to the influence of the integration scheme or the grid CFL number. While the EI scheme shows no dependency of the grid CFL number in the analyzed range, the BDF2 scheme on the other hand does. The results imply, that for the BDF2 scheme attention should be payed to the grid CFL condition.

7 ACKNOWLEDGEMENTS

This work was supported by the 'Excellence Initiative' of the German Federal and State Governments and the Graduate School of Computational Engineering at Technische Universität Darmstadt. We would like to thank Stephen Sachs for his kind cooperation that led to this work.

REFERENCES

[1] Demirdzic, I. and Peric, M. Space conservation law in finite volume calculations of fluid flow. *International Journal for Numerical Methods in Fluids* **8**, 1037–1050 (1988).

[2] Donea, J., Huerta, A., Ponthot, J.-P. and Rodríguez-Ferran, A. *Arbitrary Lagrangian–Eulerian Methods* (John Wiley & Sons, Ltd, 2004).

[3] Farhat, C., Geuzaine, P. and Grandmont, C. The Discrete Geometric Conservation Law and the Nonlinear Stability of ALE Schemes for the Solution of Flow Problems on Moving Grids. *Journal of Computational Physics* **174**, 669–694 (2001).

[4] Thomas, P. D. and Lombard, C. K. Geometric Conservation Law and Its Application to Flow Computations on Moving Grids. *AIAA Journal* **17**, 1030–1037 (1979).

[5] Geuzaine, P., Grandmont, C. and Farhat, C. Design and analysis of ALE schemes with provable second-order time-accuracy for inviscid and viscous flow simulations. *Journal of Computational Physics* **191**, 206–227 (2003).

[6] Technische Universität Darmstadt, Institute of Numerical Methods in Mechanical Engineering, Darmstadt. *FASTEST Manual* (2005).